ELSEVIER

Biochimica et Biophysica Acta 1505 (2001) 94–107

BIOCHIMICA ET BIOPHYSICA ACTA
BBA

www.bba-direct.com

Review

The Na^+-translocating F_1F_0 ATP synthase of *Propionigenium modestum*: mechanochemical insights into the F_0 motor that drives ATP synthesis[1]

Georg Kaim *

Institut für Mikrobiologie, Eidgenössische Technische Hochschule, ETH-Zentrum, Schmelzbergstrasse 7, CH-8092 Zürich, Switzerland

Received 28 July 2000; received in revised form 16 October 2000; accepted 16 October 2000

Abstract

The ATP synthase of *Propionigenium modestum* encloses a rotary motor involved in the production of ATP from ADP and inorganic phosphate utilizing the free energy of an electrochemical Na^+ ion gradient. This enzyme clearly belongs to the family of F_1F_0 ATP synthases and uses exclusively Na^+ ions as the physiological coupling ion. The motor domain, F_0, comprises subunit a and the b subunit dimer which are part of the stator and the subunit c oligomer acting as part of the rotor. During ATP synthesis, Na^+ translocation through F_0 proceeds from the periplasm via the stator channel (subunit a) onto a Na^+ binding site of the rotor (subunit c). Upon rotation of the subunit c oligomer versus subunit a, the occupied rotor site leaves the interface with the stator and the Na^+ ion can freely dissociate into the cytoplasm. Recent experiments demonstrate that the membrane potential is crucial for ATP synthesis under physiological conditions. These findings support the view that voltage generates torque in F_0, which drives the rotation of the γ subunit thus liberating tightly bound ATP from the catalytic sites in F_1. We suggest a mechanochemical model for the transduction of transmembrane Na^+-motive force into rotary torque by the F_0 motor that can account quantitatively for the experimental data.

Keywords: F_1F_0 ATP synthase; Rotational mechanism; F_0 motor; Membrane potential; Na^+ occlusion; *Propionigenium modestum*

1. Introduction

ATP, the universal biological energy currency, is formed by F_1F_0 ATP synthases from ADP and inorganic phosphate with the use of energy from a transmembrane ion potential established by photosynthetic or respiratory processes. F-type ATP synthases are widely distributed in nature and occur in the cytoplasmic membrane of bacteria, the inner membrane of mitochondria and the thylakoid membrane of chloroplasts. All known F_1F_0 ATP synthases show conserved structural and functional features and are composed of two distinct subcomplexes termed F_1 and F_0. The F_1 sector is membrane-associated and harbors the catalytic sites of ATP synthesis, while the F_0 sector is membrane-intrinsic and contains the coupling ion translocation machinery. Although most F-type ATP synthases exclusively use protons as coupling ions, the F_1F_0 ATP synthase of *Propionigenium modestum* is the prototype of a few ATP synthases that show an extended coupling ion specificity for Na^+, Li^+, or H^+ under certain conditions [35–37]. Other Na^+-translocating ATP synthases were discovered in *Acetobacterium woodii* [51] and *Ilyobacter tartaricus* [47]. The high homol-

* Fax: +41-1-6321148;
E-mail: gkaim@micro.biol.ethz.ch

[1] Dedicated to Peter Dimroth on the occasion of his 60th birthday.

0005-2728/01/$ – see front matter
PII: S0005-2728(00)00280-2

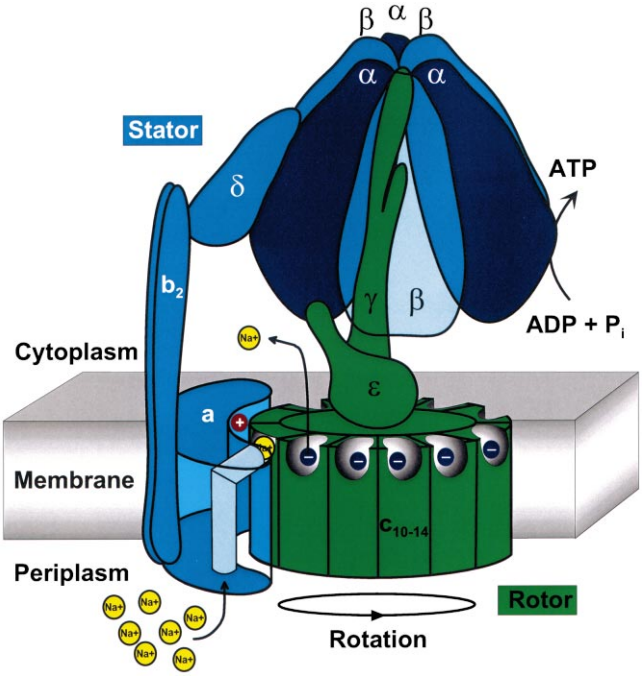

Fig. 1. Cartoon of the structure and function of the *P. modestum* F_1F_0 ATP synthase. The enzyme consists of the water-soluble F_1 domain with the catalytic sites on the three β subunits and the F_0 motor harboring the Na^+ binding sites on the c subunits and a Na^+-conducting blind channel within subunit a. F_1 is connected to F_0 via the central stalk consisting of subunits γ and ε and the peripheral stalk consisting of subunit δ and the b subunit dimer. The rotor (green) is composed of subunits $\gamma\varepsilon c_{10-14}$ and the stator (blue) comprises the $ab_2\delta\alpha_3\beta_3$ assembly. During ATP synthesis, Na^+ ions pass from the periplasm through the stator channel and occupy an empty rotor subunit. After the rotor has turned, the occupied c subunit is moved out of the interface with the stator and the Na^+ ion can dissociate into the cytoplasm. The positive stator charge (R227; red ⊕) electrostatically attracts empty negatively charged rotor sites (E65; blue ⊖) and thus contributes to torque generation required for ATP synthesis. On the other hand, ATP hydrolysis drives the rotor/stator movement in the reverse direction (not shown). Na^+ ions can board an accessible empty rotor site from the cytoplasm and exit the enzyme to the periplasm via the stator channel after the rotor has turned.

ogy between H^+- and Na^+-translocating F_1F_0 ATP synthases was demonstrated by the in vitro and in vivo construction of functional chimeras consisting of *P. modestum* F_0 and *Escherichia coli* F_1 subcomplexes suggesting that ion translocation mechanism and coupling mode are the same in all organisms [25,26,38].

The *P. modestum* ATP synthase comprises eight different subunits with a stoichiometry of $\alpha_3\beta_3\gamma\delta\varepsilon$ for F_1 and ab_2c_{10-14} for F_0 (Fig. 1). As indicated by electron micrographs, the F_1 moiety is connected to the F_0 sector via a peripheral stalk, formed by subunits δ and the subunit b dimer, and a central stalk, formed by the ε and the γ subunits [5,65]. The X-ray structure of the $\alpha_3\beta_3\gamma$ portion of bovine F_1 revealed an alternating hexagonal arrangement of three α and three β subunits around a centrally located γ subunit, which interacts asymmetrically with the catalytic β subunits [1]. Recently, an electron density map obtained from crystals of a yeast subcomplex comprising all F_1 and the c subunits of F_0 showed a ring-like arrangement of 10 c subunits which are in close contact with the central stalk units γ and ε [57]. This extensive contact provides a structural basis for the subdivision of the F_1F_0 complex into the rotor ($\gamma\varepsilon c_{10}$) and stator ($ab_2\alpha_3\beta_3\delta$) assemblies. During ATP hydrolysis, subunit γ was shown to rotate together with subunit ε relative to the three β subunits, thereby promoting tight ATP binding and ADP release [6,11,33,48,52]. The rotation of the γεc ring assembly, however, is still a matter of intensive investigation and debate. Recently, direct evidence for ATP-driven rotation of the c ring within the F_1F_0 complex of *E. coli* has been presented [53], but it was challenged by similar experiments showing that the possibility of unspecific labelling or destabi-

lizing detergent effects cannot be excluded with certainty [61]. Another approach seems to circumvent these criticisms by connecting biotinylated, fluorescent actin filaments via streptactin to a genetically engineered 'strept tag' at the N-terminus of subunit c and ATP-driven rotation of actin filaments could be directly visualized using the microvideography technique [49].

During ATP hydrolysis, F_1F_0 ATP synthases act as ion pumps and the rotation of the rotor would force cytoplasmic Na^+ ions (or protons) to pass via the rotor binding sites through the stator channel to the periplasmic side of the membrane. However, in its reverse operation the most interesting question is how the F_0 motor converts the energy stored in a transmembrane electrochemical ion gradient into rotary torque necessary for ATP formation (for reviews see [2,8,9,13,42]). Recent experiments demonstrate that the ATP synthases of chloroplasts, like those of mitochondria and bacteria, require a membrane potential for ATP synthesis [30–32]. Thus, voltage plays a crucial role in the rotary catalysis mechanism. In this review, we will emphasize experimental data that have helped to design a molecular model describing some aspects of the torque-generating process that drives the rotation of the c subunits versus subunit a in the F_0 motor.

2. Organization and function of the F_0 sector

In contrast to the detailed structural information available for the F_1 part, little is known about the structural details of F_0. Electron spectroscopic imaging and atomic force microscopy together with recent X-ray crystallography data of the mitochondrial yeast F_1c subcomplex suggest an overall structure of F_0 consisting of a ring of c subunits which is flanked on one side by the a and the two b subunits [3,55,57,59]. Interestingly, the stoichiometry of c subunits in the ring varies. The c ring of yeast consists of 10 monomers [57], whereas in chloroplasts 14 c subunits are assembled into a cylindrical ring [54]. Moreover, cross-linking and genetic studies in *E. coli* have been interpreted as showing the presence of 12 c subunits per F_0 [22]. Monomeric subunit c is a small hydrophobic membrane protein which is also called proteolipid due to the observation that it can be isolated in organic solvent mixtures. The c subunits of different organisms comprise 70–90 amino acids with molecular masses between 8 and 10 kDa and are thus ideal objects for structure determinations using nuclear magnetic resonance (NMR) techniques.

The structure of *E. coli* subunit c has been determined by NMR in chloroform:methanol:water (4:4:1) at pH 5.0 and pH 8.0 [15,50]. Comparison of the two structures revealed that the monomeric subunit c of *E. coli* adopts a hairpin-like fold and packs into two antiparallel α-helices of 38 and 33 residues, respectively, which are connected by a polar loop of six or seven amino acids. The main difference in the two structures is a 140° rotation of the C-terminal helix with respect to the N-terminal helix. Upon modelling these structures into the membrane, the H^+ binding Asp^{61} residue (Glu^{65} in *P. modestum*) was placed into the center of the bilayer [13]. However, experimental evidence for this location is not available. In a membrane-buried position, the binding sites are occluded and direct access of the coupling ion from either side of the membrane is not feasible. Since both α-helices are too long to completely insert into the membrane bilayer, alternative membrane boundaries of the protein are conceivable as well. Thus, the critical Asp^{61} residue could also be located more closely to the membrane surface where it could have direct access to the coupling protons. This suggestion was supported by epitope mapping of monoclonal antibodies prepared against subunit c of *E. coli* demonstrating that the region between positions 31 and 42 is accessible from the cytoplasm [4]. Moreover, cross-link experiments between subunits a and c showed that the C-terminal helix of subunit c starts near position 54 [21]. In summary, these results indicate that the surface loop region of *E. coli* subunit c comprises at least residues 31–54 (residues 35–58 in *P. modestum* subunit c) and protrudes into the cytoplasm with a greater expansion as deduced from the NMR structures.

In contrast to the c subunit of *E. coli*, the *P. modestum* c subunit precipitates in the monophasic organic solvent mixture within several hours. However, isolated *P. modestum* c subunit assumes a temperature-stable, highly α-helical structure in dodecyl sulfate micelles as evidenced by circular dichroism in the temperature range between 20 and 60°C [43].

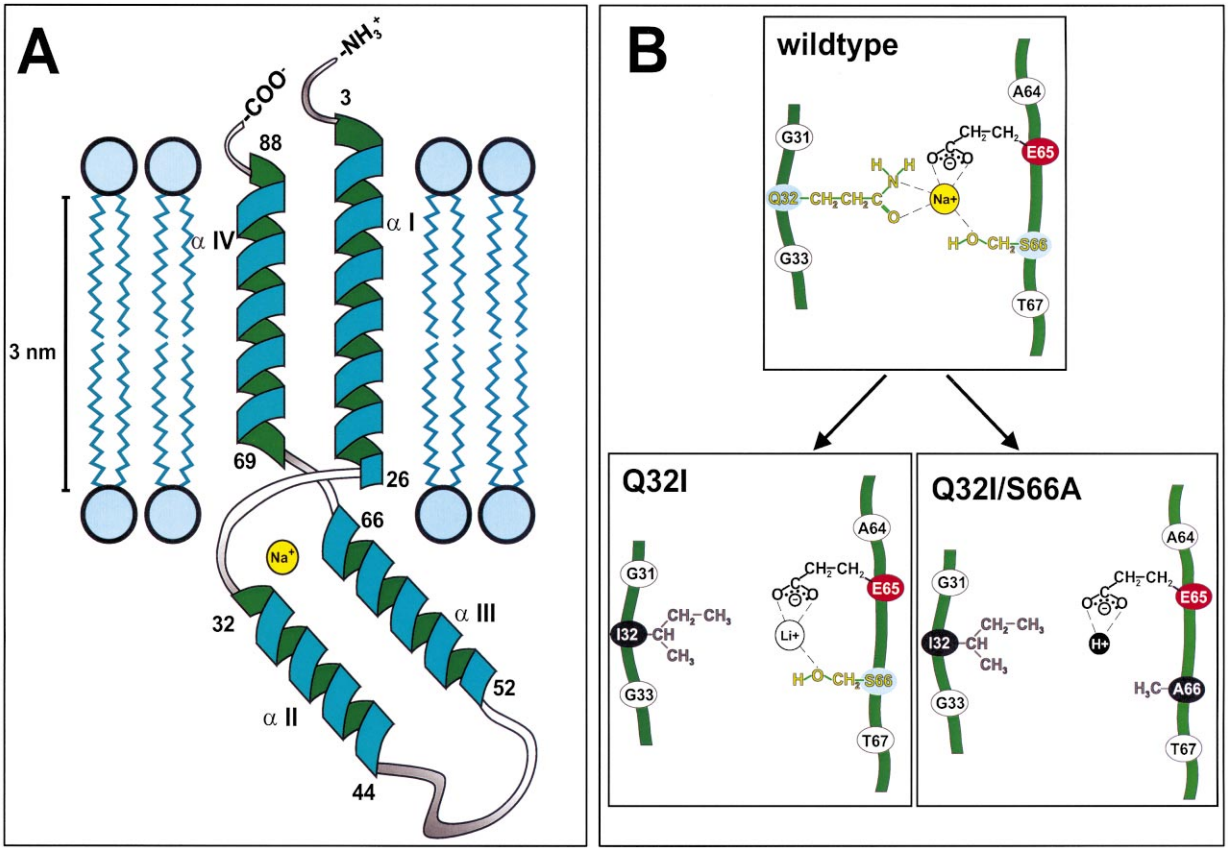

Fig. 2. (A) Model for the membrane insertion of subunit c. Helices I (24 residues) and IV (18–20 residues) of the *P. modestum* c subunit span the membrane, whereas helices II (13 residues) and III (15 residues) and the connecting loop (seven residues) are exposed to the cytoplasm. The Na^+ binding site comprises the triad Gln^{32}, Glu^{65}, and Ser^{66} in the interhelical region between helices I/II and III/IV, and could be located near the cytoplasmic surface of the membrane. (B) Details of the coupling ion coordination sphere of the *P. modestum* c subunit. In the wild-type, the binding of Na^+ ions requires ligands contributed by Gln^{32}, Glu^{65} and Ser^{66}. In the Gln^{32}Ile mutant, Na^+ liganding was completely abolished, whereas Li^+ or H^+ binding was retained. Upon the additional replacement of Ser^{66} by Ala, no Na^+ or Li^+ coordination was detected and Glu^{65} is the only residue for H^+ binding and translocation in the Gln^{32}Ile/Ser^{66}Ala double mutant.

NMR structure determinations of the *P. modestum* c subunit were therefore performed in dodecyl sulfate micelles mimicking more closely the biphasic character of the membrane bilayer [44]. The structure comprises four clearly defined α-helical domains that are interrupted in the vicinity of the Na^+ binding site by short peptides with non-α-helical structure and by the polar loop (Fig. 2A). The N- and C-terminal α-helices I and IV are the best structured and the most stable parts of this protein. These segments include 24 and 20 amino acids, respectively, and are thus long enough to span the membrane. The additional helices II (12 residues) and III (14 residues) and the polar loop (eight residues) were proposed to protrude into the cytoplasm. In this structure, the triad of Na^+ binding residues, cQ32, cE65 and cS66, is located within the helix I→II and III→IV connections probably close to the cytoplasmic membrane boundary, where direct access of the coupling ions is feasible.

Given that structures of homologous proteins have been conserved during evolution, the different NMR structures determined for the c subunits of *E. coli* and *P. modestum* are hard to reconcile. An obvious explanation would be that the two proteins are differently folded in the organic solvent mixture or in the detergent micelles. It has been suggested that the structure of monomeric *E. coli* subunit c resembles that in the native F_0 complex, because the modification of Asp^{61} by *N,N′*-dicyclohexylcarbodiimide (DCCD) was retained [14]. The finding that the mod-

ification rate of monomeric subunit c was reduced by four orders of magnitude when compared to the modification rate of *E. coli* F_1F_0, however, demands critical reflection on this conclusion. On the other hand, the initial rate of DCCD modification of the *P. modestum* c monomer was approximately 100-fold lower than in the F_1F_0 complex, and Na^+ provided partial protection from DCCD modification indicating that the Na^+ binding site is retained to some extent [43]. In order to finally corroborate which of these monomeric c subunits reflects a native folding pattern, additional structural information enclosing the entire F_0 sector is needed.

Importantly, subunit c plays a key function in ion binding and release during coupling ion translocation across the F_0 sector. This implies the presence of a binding site on subunit c that specifically recognizes the coupling ions and it could be demonstrated that *P. modestum* F_0 specifically binds Na^+ or H^+ if the Na^+ concentration is low (<1 mM) [37]. Further experiments revealed that subunit c is responsible for Na^+ or H^+ recognition and may additionally bind Li^+ ions albeit the Li^+ concentration to achieve half-maximal activation of ATP hydrolysis is 10-fold higher than the Na^+ concentration [35,36]. The Na^+ binding ligands consist of Gln^{32}, Glu^{65}, and Ser^{66} and were identified by a mutagenesis approach targeted to the *P. modestum* c subunit (Fig. 2B) [27]. Upon $Gln^{32}Ile$ replacement the Na^+-dependent properties were completely abolished while Li^+ and H^+ binding was retained. If Ser^{66} was additionally exchanged to alanine, the binding specificity of the $Gln^{32}Ile/Ser^{66}Ala$ double mutant was restricted to H^+ as the exclusive coupling ion. These results demonstrate that cQ32, cE65 and cS66 are essential for Na^+ binding, while cE65 and cS66 accommodate Li^+ binding and cE65 is sufficient to accomplish H^+ binding and release [27]. Consistent results were derived from mutagenesis studies performed in the vicinity of the conserved Asp^{61} residue of *E. coli* subunit c, which is equivalent to *P. modestum* Glu^{65}. By mutating the *E. coli* residues around Asp^{61} to the corresponding *P. modestum* residues a Li^+ binding site was created [67]. As expected from the absence of the Na^+-liganding Gln^{32} residue, Na^+ binding could not be detected.

Structural information on the a subunit, a very hydrophobic membrane-integral protein, is limited and recent topological models that anticipate five or six membrane-spanning helices have been derived [19,41,63,66]. Briefly, all models suggest a similar topological arrangement of the two C-terminal α-helices and from mutation studies it was proposed that this domain participates in the translocation of the coupling ions [7,39,40]. The helices could be packed to permit a channel that is open to the periplasmic side and closed to the cytoplasmic side. Importantly, only Arg^{227} (*P. modestum* numbering) is highly conserved among all species investigated and even conservative replacements at this position completely abolish ATP synthesis [17]. According to the topology of subunit a, Arg^{227} is located near the cytoplasmic surface of the membrane where it can electrostatically interact with Glu^{65} of subunit c (Fig. 1).

Subunit b is an amphipathic protein consisting of a hydrophobic N-terminal segment of about 30 amino acids that most likely forms a transmembrane α-helix which anchors the protein in the membrane. The C-terminal domain is hydrophilic, mainly α-helical, and protrudes from the membrane into the cytoplasm. Cysteine scanning mutagenesis performed with the hydrophilic portion of *E. coli* subunit b showed that the domain between positions 124 and 146 constitutes an essential contact site for homodimer formation, also evidenced by the finding that $Val^{124}Asp$ or $Ala^{128}Asp$ replacement dissects the dimer into monomers [18,45]. The elongated C-terminus of the subunit b dimer is essential for the connection of F_0 with F_1 presumably via subunit δ. Experimental evidence in favor of this function was obtained from proteolysis studies of F_0 and removal of two residues from the C-terminus completely prevented F_1F_0 assembly [56,58].

3. Translocation of the coupling ions through F_0 requires rotation of the c subunit oligomer versus subunit a

An important prerequisite for ion translocation across the F_0 sector is the presence of discrete coupling ion binding sites and compelling evidence has been accumulated that subunit c is provided with specific ligands accomplishing this function [27]. Experimental support that the Na^+ specificity of the *P.*

modestum ATP synthase was also determined by structural elements of subunit a could recently be obtained by a genetic approach. After random mutagenesis of the *P. modestum* F_0 genes, a triple mutant in subunit a ($Lys^{220}Arg$, $Val^{264}Phe$, $Ile^{278}Asn$) could be isolated in which Na^+ translocation was abolished, but Li^+ and H^+ translocation was retained [29]. Interestingly, ATP hydrolysis of the mutant enzyme was specifically inhibited by Na^+, whereas the wild-type ATPase was activated by Na^+. This demonstrates that the Na^+ binding sites on the c subunits remained intact and were not affected by the subunit a triple mutation. In addition, subunit a could contribute an ion-selective channel which has become Na^+-impermeable by mutation. Since ATP hydrolysis is strictly coupled to ion pumping in the F_1F_0 complex, the ATPase activity should stop if the Na^+ pathway through the F_0 sector is blocked. This idea was further pursued by $^{22}Na^+$ labeling experiments of the triple mutant ATP synthase and it was shown that 1 mol of $^{22}Na^+$ was occluded per mol of the mutant ATPase in a strictly ATP-dependent manner [28]. In contrast, $^{22}Na^+$ occlusion could not be observed in the presence of ADP or AMP-PNP, a non-hydrolyzable ATP analogue, or with the wild-type ATPase containing a Na^+-permeable subunit a channel. The stoichiometry of one Na^+ occluded per mutant ATPase shows that all binding sites at the c subunits are freely accessible for the Na^+ ions from the aqueous environment with the exception of that c subunit at the subunit a interface. This is in accord with the proposal that one channel is present on subunit a and conflicts with models that anticipate two subunit a half-channels which are connected by an uninterrupted chain of Na^+-occupied c subunits [11,12,24,50,64]. Such a model implies that $^{22}Na^+$ enters its binding site, which is buried in the middle of the membrane bilayer, through one stator half-channel and leaves the enzyme through the other half-channel after almost a complete revolution of the rotor. In the triple mutant, ATP-driven rotation would immediately stop if a $^{22}Na^+$-occupied c subunit reaches the interface to the Na^+-impermeable release channel. As a consequence, all c subunits between the two half-channels should be boarded with their coupling ion and approximately 10 $^{22}Na^+$ would thus be captured within the enzyme. However, such a stoichiometry has not been observed experimentally.

First evidence for revolutions of the rotor versus the stator was also obtained from $^{22}Na^+$ occlusion experiments performed with the mutant ATPase after destroying part of the Na^+ binding sites on subunit c by chemical modification with DCCD [30]. The rationale behind this was to create an F_0 motor whose rotation can be blocked either through the mutated stator or through a modified rotor subunit. Importantly, one $^{22}Na^+$ was occluded per mutant ATPase if $^{22}Na^+$ was added first and ATP second. However, no $^{22}Na^+$ was occluded if this sequence of additions was reversed. These results can easily be explained by the rotational mechanism: in the first case, ATP-driven rotation stops and $^{22}Na^+$ becomes occluded when a Na^+-loaded rotor subunit has been moved into contact with the Na^+-impermeable stator channel. In the second case ATP-driven rotation stops without $^{22}Na^+$ occlusion when a DCCD-modified rotor subunit strikes against the stator (Fig. 3). Thus, a mechanism that accounts for ATP-driven ion transport through the F_0 sector of F-type ATPases requires specific binding sites on the rotor subunits which are freely accessible from the cytoplasm and one water-filled stator channel which connects a rotor binding site to the periplasm. First, Na^+ ions approaching their rotor binding site from the cytoplasm would strip off their water shell and become liganded by cQ32, cE65 and cS66. The geometry of the liganding residues determines the coupling ion specificity of the enzyme and represents the structural basis of the so-called selectivity filter. Second, ATP drives the rotation of the rotor versus the stator and moves a Na^+-occupied rotor site into the rotor/stator interface where it contacts the Na^+-selective stator channel. This rotatory movement disconnects the occupied binding site from the cytoplasmic side of the membrane and connects it with the periplasmic membrane side. Third, the Na^+ ion dissociates from the rotor site into the stator channel and leaves the enzyme upon rehydration to the periplasmic side of the membrane.

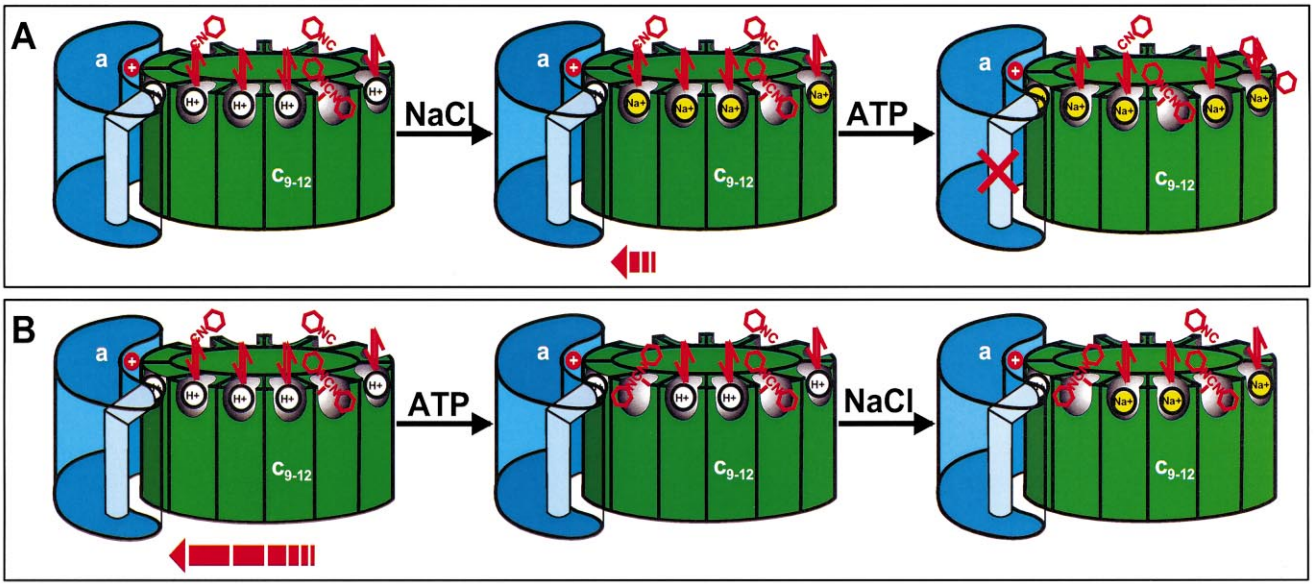

Fig. 3. Rotational events during $^{22}Na^+$ occlusion by the F_0 motor. In the absence of NaCl, the rotor subunits are in free equilibrium with H^+. (A) If $^{22}NaCl$ was added, the rotor subunits are immediately occupied by Na^+ ions. Upon ATP addition the rotor turns and moves an occupied rotor subunit into the stator boundary. Since the stator channel is blocked by mutation, the coupling ions cannot exit the enzyme and one $^{22}Na^+$ was trapped per ATP synthase. (B) If ATP was added, the rotor turns and a DCCD-modified rotor subunit strikes against the stator. Once kept in this immobilized position, no occlusion occurred upon the addition of $^{22}NaCl$.

4. Operation modes of the F_0 module: ion pump, motor for ATP synthesis or ion shuttle

The concept described above implies that the F_0 subcomplex is mechanistically comparable with a pumping device that is propelled by the ATP-powered F_1 engine unit. Upon hydrolyzing ATP, the released energy is transmitted from the F_1 moiety via a rotating eccentric shaft (γ subunit) to the F_0 sector which performs osmotic work by translocating the coupling ions from the cytoplasmic to the periplasmic membrane side. In the reverse direction, the F_0 part operates as an ion-powered motor by using the energy stored in an electrochemical ion gradient for the generation of rotary torque that drives ATP synthesis at the F_1 subcomplex.

A third operation mode of the F_0 module was discovered in the absence of an external driving force. Under these conditions, the F_0 motor is in its idling mode and the rotor might perform Brownian back and forth movements versus the stator within a narrow angle. After reconstitution of the entire *P. modestum* F_1F_0 complex or the F_0 sector into proteoliposomes containing 2 mM $^{22}NaCl$ on the outside and 100 mM NaCl on the inside, a rapid exchange of external $^{22}Na^+$ against internal unlabelled Na^+ could be measured [30]. $^{22}Na^+_{out}/Na^+_{in}$ exchange was catalyzed with an initial rate of 7 s^{-1}, which corresponds to the initial rate of 8 s^{-1} obtained for ATP-driven Na^+ pumping. This indicates that idling characterizes a reaction step which is not artificial, but significantly related to the common ion translocation mechanism under catalytic conditions. In the idling mode, the F_0 module behaves like an ion shuttle that exchanges Na^+ ions between the two aqueous compartments separated by the membrane (Fig. 4). If an external $^{22}Na^+$ ion binds to its rotor site, this rotor subunit could enter the stator interface. Once in contact with the stator, the rotor subunit is discharged and the released $^{22}Na^+$ ion reaches the internal lumen through the stator channel. The same rotor site, now empty, would pick up an unlabelled internal Na^+ ion from the stator channel and moves backwards, out of the stator interface. Thus, the rotor subunit gains access to the external side again and the bound Na^+ ion dissociates.

Interestingly, the $^{22}Na^+_{out}/Na^+_{in}$ exchange was not significantly affected by modifying part of the rotor sites with DCCD. This is in accord with F_0 models involving one channel on the stator as illustrated in

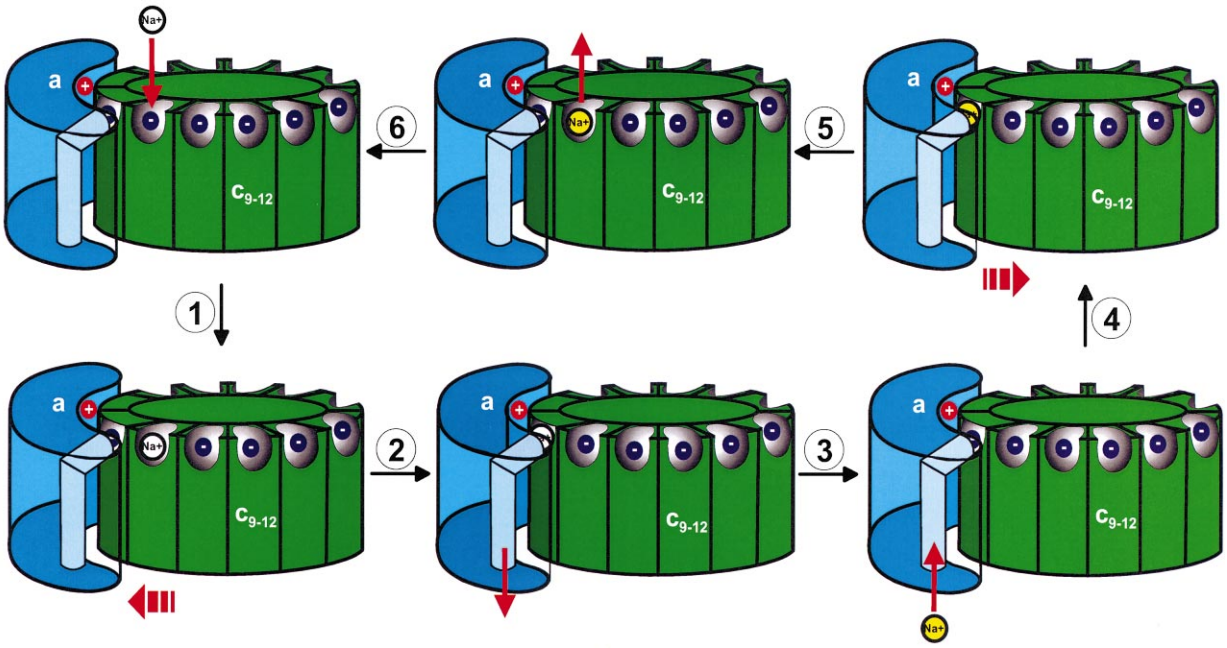

Fig. 4. Schematic representation of $^{22}Na^+_{out}/Na^+_{in}$ exchange catalyzed by the reconstituted F_0 motor. (1) A $^{22}Na^+$ ion (white) occupies its binding site from the external side of the proteoliposomes. (2) Limited forth rotation of the rotor versus the stator moves the occupied rotor site into the stator boundary. (3) The $^{22}Na^+$ ion is released via the stator channel into the lumen of the proteoliposomes. (4) The empty rotor site picks up an unlabelled Na^+ ion (yellow) from the luminal side of the proteoliposomes. (5) The re-occupied rotor site departs the stator boundary by limited back rotation and gains access to the external membrane side. (6) The unlabelled Na^+ ion is released and the empty rotor is available for another exchange reaction.

Fig. 4. In such an assembly, the observed exchange reaction can be explained by rotor/stator revolutions that could occur within an angle of approximately 30–60° restricted by the limited flexibility of subunit γ. In contrast, models with two half-channels on the stator would require an almost complete rotation of the rotor versus the stator to realize the exchange reaction itself. In those 'two-channel models' the negatively charged rotor binding sites are centered in the middle of the membrane and must be neutralized by their coupling ions. If this chain of occupied binding sites was interrupted by DCCD modification and a rotor site was loaded via one half-channel it would be impossible for this occupied rotor site to reach the second half-channel. Thus, in contrast to the observed experimental data, idling would be abolished by DCCD modification.

It is obvious that the F_0 motor has to switch from the idling mode, characterized by $^{22}Na^+_{out}/Na^+_{in}$ exchange, into a unidirectional rotation mode to perform ion pumping or to generate torque. Ion pumping was achieved by ATP hydrolysis in the F_1 module which drives the rotary movement of the rotor assembly. Upon ATP addition to the idling F_1F_0 ATPase with partially DCCD-modified rotor subunits, $^{22}Na^+_{out}/Na^+_{in}$ exchange was completely abolished [30]. This could be explained if the rotor turns during ATP hydrolysis and a DCCD-modified rotor site strikes against the stator. In this immobilized position the rotor is unable to perform Brownian motion against the stator and no $^{22}Na^+_{out}/Na^+_{in}$ exchange is catalyzed. In the ATP synthesis direction, the F_0 module must utilize the energy of an electrochemical ion gradient for torque generation. Unexpectedly, during idling $^{22}Na^+$ uptake was observed against a Na^+ concentration gradient ($\Delta pNa^+ \approx 100$ mV) indicating that ΔpNa^+ is apparently unable to generate torque and is thus not a suitable driving force for ATP synthesis. However, if a membrane potential ($\Delta\Psi$) of ~90 mV was applied, the F_0 module switched from idling into the torque-generating operation mode and $^{22}Na^+_{out}/Na^+_{in}$ exchange was completely prevented [30]. This significant result complements previous findings with the

isolated F_0 sector [34]. The F_0 module alone catalyzed efficient $^{22}Na^+_{out}/Na^+_{in}$ exchange but was unable to perform Na^+ uptake in response to a ΔpNa^+ of −180 mV. Moreover, Na^+ transport was strictly dependent on size and direction of the $\Delta\Psi$ and significant uptake rates were only observed with electric potentials above −40 mV [34]. Thus, the idling F_0 sector either isolated or combined with the F_1 subcomplex performs limited rotational movements of the rotor against the stator and shuttles Na^+ ions back and forth across the membrane. This mobility persists even in the presence of a large Na^+ concentration gradient which is therefore unable to switch the F_0 sector from the idling into the torque-generating mode. In contrast, voltage induces this switch and replaces $^{22}Na^+_{out}/Na^+_{in}$ exchange by $\Delta\Psi$-driven Na^+ transport. The direction of rotation depends on the sign of the membrane potential and determines the route of Na^+ transport. With reconstituted F_0, this transport can be directly followed because in the isolated F_0 motor the rotor can freely rotate into either direction. In the F_1F_0 ATP synthase, however, $\Delta\Psi$-driven Na^+ accumulation was not observed because the free rotation of the rotor is arrested by the F_1 module. To acquire rotation, this system must therefore be supplied with Mg-ADP and inorganic phosphate in order to synthesize ATP and to relieve the constraints for a continuous rotation of the γ subunit within the F_1 headpiece.

5. The membrane potential is kinetically indispensable for ATP synthesis

The idea that the electric potential ($\Delta\Psi$) plays a mandatory role in switching the F_0 motor from idling into torque generation clearly implies that voltage constitutes the obligatory driving force for ATP synthesis. This was corroborated by investigating the relative contribution of $\Delta\Psi$ and $\Delta pNa^+/\Delta pH$ on ATP production catalyzed by three different ATP synthases reconstituted into liposomes [30–32]. No ATP formation was observed with the ATP synthases of *P. modestum*, *E. coli*, or spinach chloroplasts if only ΔpNa^+ or ΔpH were applied as the driving force. However, in the presence of a membrane potential, the rate of ATP synthesis increased exponentially with increasing $\Delta\Psi$ approaching maximal rates at $\Delta\Psi = 70$ mV for the chloroplast enzyme and at $\Delta\Psi = 120$ mV for the bacterial ATP synthases (Fig. 5). Half-maximal activities for the *P. modestum* and *E. coli* enzymes were obtained at $\Delta\Psi = 70$ mV and at $\Delta\Psi = 35$ mV for the chloroplast ATP synthase. The low membrane potential necessary for activation of the chloroplast enzyme could account for an adaptation to the minimal $\Delta\Psi$ (≤50 mV) observed in chloroplasts during permanent illumination, i.e. under steady-state conditions [16]. Remarkably, if a substantial $\Delta pNa^+/\Delta pH$ was additionally applied, the ATP synthesis rate increased, but to a

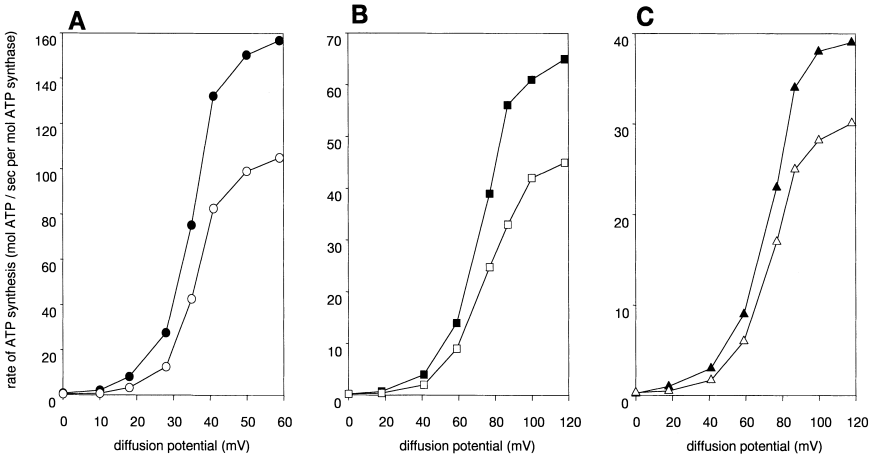

Fig. 5. Relative contribution of the electric potential ($\Delta\Psi$) and the H^+ or Na^+ concentration gradient (ΔpH; ΔpNa^+) on the rate of ATP formation by three different F_1F_0 ATP synthases. (A) Reconstituted chloroplast ATP synthase. K^+/valinomycin diffusion potentials were applied in the absence (○) or presence (●) of $\Delta pH = 206$ mV. (B) Reconstituted *E. coli* ATP synthase. K^+/valinomycin diffusion potentials were applied in the absence (□) or presence (■) of $\Delta pH = 206$ mV. (C) Reconstituted *P. modestum* ATP synthase. K^+/valinomycin diffusion potentials were applied in the absence (△) or presence (▲) of $\Delta pNa^+ = 77$ mV.

lesser extent than expected if $\Delta pNa^+/\Delta pH$ and $\Delta\Psi$ were kinetically equivalent driving forces. This indicates that $\Delta\Psi$ is indispensable as a driving force for ATP production in F-type ATP synthases and cannot be replaced by $\Delta pNa^+/\Delta pH$ for kinetic reasons.

According to Mitchell's chemiosmotic theory, $\Delta\Psi$ and ΔpH are thermodynamically equivalent driving forces [46]; however, the contribution of either component to the kinetics of ATP synthesis may vary in different organisms. In bacteria, $\Delta\Psi$ is a more valuable driving force for ATP synthesis than ΔpH, since it ensures physiological flexibility during the response to frequently changing pH values in their environment. Extreme species like the alkaliphiles or the acidophiles grow at pH values above 10 or below 4, respectively, whereas the internal pH must be maintained around 8.5. Thus, in alkaliphiles $\Delta\Psi$ is not only the driving force for ATP synthesis, but must also compensate for the inwardly directed ΔpH. Similarly, the proton-motive force in mitochondria primarily consists of $\Delta\Psi$ and to a lesser extent of ΔpH suggesting that the membrane potential constitutes the main driving force for ATP synthesis in these organelles [60]. In contrast, important early studies describe ATP synthesis in chloroplasts after energization of the thylakoid membranes with ΔpH only [20]. Numerous investigations performed with the reconstituted chloroplast ATP synthase and other sources analyzed the quantitative contribution of $\Delta\Psi$ and ΔpH on ATP synthesis and seemed to indicate that ΔpH and $\Delta\Psi$ are not only thermodynamically but also kinetically equivalent driving forces [23,62].

The reason for these contradictory results is an intrinsic feature of the 'acid bath procedure' introduced by Jagendorf and Uribe [20], which has been widely used to study the response of ATP synthases on ΔpH. As outlined in Fig. 6, the vesicles were first incubated with 10 mM succinate, pH 4–5, which acidifies the internal lumen. The pH gradient was then generated by rapid 1:1 dilution of the suspension into Tris buffer, pH 8.5, containing ADP and inorganic phosphate, and ATP synthesis was monitored. Recently, it was shown that this procedure establishes not only the desired ΔpH, but could also generate a $\Delta\Psi$ of substantial size due to the diffusion of the monovalent succinate species [32]. After the basic transition the concentration of the

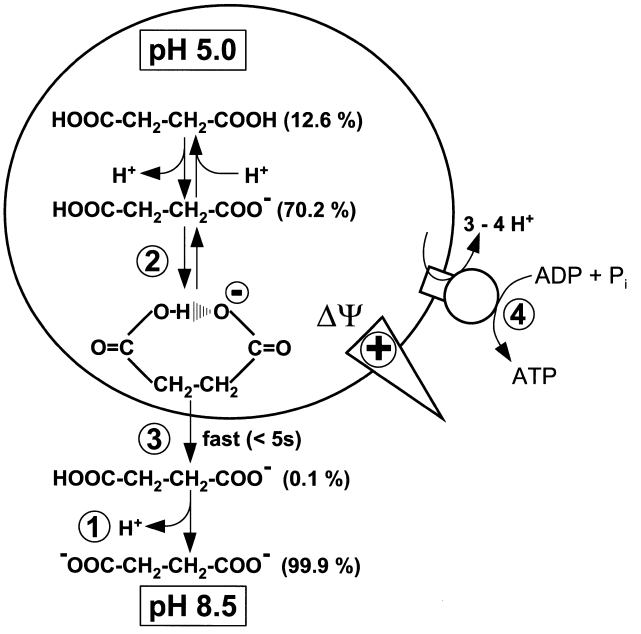

Fig. 6. Generation of a membrane potential by the 'acid bath procedure'. During the acid stage, the proteoliposomes are equilibrated with 10 mM succinate buffer, pH 5.0. At this pH 70.2% of the succinate is present as monoanion. At the basic stage, the external pH is shifted to 8.5 by a 1:1 dilution of the proteoliposome suspension with 100 mM glycylglycine buffer, pH 8.5. This pH jump shifts the equilibrium of external succinate towards the dianion (99.9%), resulting in a large concentration gradient of the succinate monoanion across the membrane (1). The succinate monoanion predominating in the internal compartment folds partially into a ring. This form is membrane-permeable because the negative charge has been delocalized between both carboxylic groups (2). Diffusion of this monoanionic succinate species from the inside to the outside following its concentration gradient generates an electric potential according to the Nernst equation (3). This potential is essential to drive ATP synthesis by proteoliposomes reconstituted with bacterial or the chloroplast ATP synthases (4).

succinate monoanion is 7.2 mM on the inside (acidic pH) and 0.006 mM on the outside (alkaline pH). The diffusion of the succinate monoanion across the membrane could generate a Nernst potential of 180 mV. This is compatible with membrane potentials of about 140 mV determined after the acid–base transition using [^{14}C]thiocyanate as the membrane-permeable probe. Further support comes from investigations on the membrane permeability of various dicarboxylic acids either by efflux of their monoanionic species or by uptake in response to $\Delta\Psi$. Similar permeabilities could be observed for succinate, malonate, malate or maleinate at the pH where the

monoanionic species prevails, whereas fumarate is apparently unable to diffuse across the membrane [32]. Upon correlating the chemical properties of the dicarboxylic acids with the membrane permeability, a remarkable difference exists between maleinate with a *cis* and fumarate with a *trans* double bond. Since only maleinate is membrane-permeable, a reasonable explanation is folding of the appropriate monoanionic species into a ring while traversing the membrane. Thus, the negative charge is delocalized to both carboxylic groups and the dielectric barrier of the membrane for the crossing monoanion decreases. On the other hand, carboxylic acids that cannot adopt a stable ring structure within the membrane carry a localized negative charge and are thus membrane-impermeable.

6. Model for torque generation in the F_0 motor

Summarizing the experimental results described in the previous sections a model of the F_0 motor was designed by Oster and colleagues [10]. As depicted in Fig. 7A, the F_0 motor is composed of the rotor and the stator. The rotor has the appearance of a symmetrically assembled ring consisting of 10–14 c subunits and encloses the freely accessible Na^+ binding sites (Q32, E65 and S66) which are located near the cytoplasmic surface of the membrane. The stator a subunit interacts laterally with the rotor and provides the essential asymmetry required for unidirectional rotation by a Na^+-selective blind channel conducting the coupling ions from the periplasmic reservoir to their binding sites on the rotor. The stator channel is connected to the cytoplasm via a horizontal hydrophilic strip which is sealed by the universally conserved positive stator charge (R227) in order to prevent ion leakage between the two aqueous reservoirs (Fig. 7B). Whereas the major part of the rotor/stator interface represents a hydrophobic barrier, the hydrophilic strip permits negatively charged (unoccupied) rotor sites to enter the rotor/stator boundary from the right and to pass as far as to the left edge of the stator channel. Rotor sites approaching the stator are likely to be empty because of two reasons: (i) the rotor sites are in dissociation equilibrium with the low Na^+ concentration of the cytoplasm and (ii) if an occupied rotor site enters the stator, the positive charge R227 will reduce the binding affinity of the rotor site and thus promote dissociation of the Na^+ ion into the cytoplasmic reservoir. Moreover, the positively charged R227, which has been placed in close vicinity to the hydrophilic strip, could promote electrostatic attraction of negatively charged rotor sites when they enter the rotor/stator interface. Another structural element that contributes to asymmetry within the stator and restricts rotor diffusion is the hydrophobic barrier at the left edge of the stator channel (Fig. 7B). Unoccupied rotor sites are prevented from crossing this electrostatic barrier because their negative charge is repelled. However, after binding a Na^+ ion from the channel, the negative charge is reduced to a dipole facing only a small electrostatic barrier, which can easily be traversed. If the occupied rotor site exits the stator to the left, the ion can dissociate into the cytoplasm. The rotor site, now negatively charged again, is hampered from rotating backwards and progression of the rotor is ratcheted. In summary, the ion pathway across the F_0 motor is from the periplasm through the stator channel onto an empty rotor site, from which the ion can dissociate into the cytoplasm after the rotor has turned.

A fundamental question is how the ion flux is coupled to the generation of rotary torque and what may be the fundamental role of $\Delta\Psi$ in the torque-generating mechanism. Basically, the movement of the rotor is stochastic due to random Brownian motion, however, electrostatic effects bias its diffusion to the left. An empty rotor site whose negative charge, E65, is electrostatically attracted by the positive stator charge, R227, is kept within its potential well (Fig. 7C). If this site is captured it can escape by thermal fluctuations. In the absence of $\Delta\Psi$ it escapes to the right or to the left with equal probabilities. However, upon applying a membrane potential, most of the voltage drop will be across the horizontal hydrophilic strip of the stator channel. This would bias the thermal escape of the rotor site from its potential well to the left, where it enters the vertical channel part and quickly binds a Na^+ ion. When occupied by a Na^+ ion, the electrostatic field of the rotor charge is reduced to a dipole and can be regarded as almost neutral. This has the dual effect that backward attraction by the stator charge is prevented and traversing the hydrophobic barrier to the

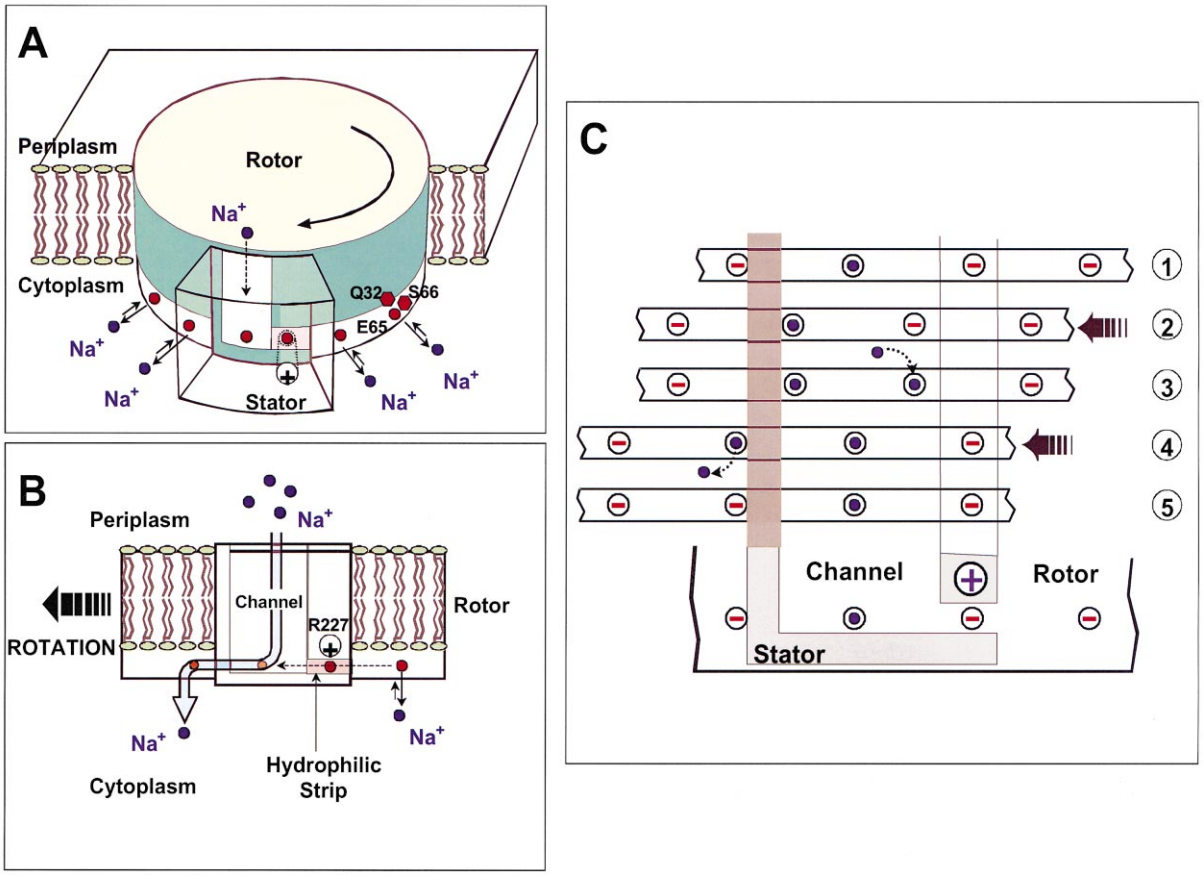

Fig. 7. Model for torque generation in the F_0 motor. (A) Illustration of the rotor/stator assembly of the *P. modestum* ATP synthase. The rotor contains 10–14 Na^+ binding sites near the cytoplasmic membrane surface. The stator is equipped with an aqueous channel that conducts ions from the periplasmic reservoir to the level of the rotor sites. This channel is laterally connected by a hydrophilic strip and ion leakage along this strip to the cytoplasm is prevented by the positive stator charge (R227). (B) Face-on view of the rotor/stator assembly. Rotation during ATP synthesis is to the left. The stator channel admits Na^+ ions from the periplasm, but they can only exit to the cytoplasm by boarding a rotor site and passing through the dielectric barrier forming the left wall of the channel. (C) Typical sequence of events that advances the rotor by one step. In position (1) the third rotor site from the left is captured by the stator charge. (1)→(2): The rotor site can escape by thermal fluctuations and the membrane potential biases its thermal escape to the left. However, it cannot pass the hydrophobic barrier that forms the left edge of the channel. (2)→(3): Once the site has moved out of the potential well towards the channel it picks up a Na^+ ion which prevents its backwards attraction by the stator charge. (3)→(4): Neutralized, the site no longer sees the hydrophobic barrier and can diffuse to the left. This movement is supported by the capture of the next empty rotor site by the stator charge, which pulls the rotor to the left. (4)→(5): Leaving the hydrophobic stator interface, the rotor site loses its ion to the cytoplasm. Now charged, it cannot diffuse backwards across the hydrophobic barrier and the thermal motion to the left is ratcheted [10].

left is permitted, if the next negatively charged rotor site is electrostatically attracted by the positive stator charge. Upon exiting the stator to the left, the occupied rotor site can discharge its ion to the cytoplasm. Once empty, the negatively charged binding site again encounters the dielectric barrier of the stator and cannot diffuse back to the right.

As described in Section 5, ATP synthesis by F-type ATP synthases is obligatorily dependent on the membrane potential [32]. In terms of our model, $\Delta\Psi$ plays a vital role in biased diffusion and elicits the thermal escape of a negatively charged rotor site from its potential well. It acts like a 'power stroke' and is absolutely essential for the generation of rotary torque within the F_0 motor. In contrast to this principal role of $\Delta\Psi$ in ATP synthesis, $\Delta pNa^+/\Delta pH$ could be involved in 'fine tuning' of the ATP synthesis rate. A high periplasmic concentration of the coupling ions

accelerates rotation since an escaped rotor site is more frequently occupied which facilitates progression through the hydrophobic barrier on the left. Similarly, rotation is accelerated if the cytoplasmic concentration of the coupling ions is low because the rotor sites are mainly empty and are thus more often attracted by the positive stator charge. It should be noted that Oster and colleagues analyzed the motor's performance by quantitative simulations. The solution of model equations demonstrates that the sodium ion F_0 motor of *P. modestum* generates sufficient torque for the synthesis of ATP [10]. The rotation is driven almost completely by the membrane potential, whereas the chemical gradient plays only a minor role in the torque-generating mechanism.

References

[1] J.P. Abrahams, A.W. Leslie, R. Lutter, J.E. Walker, Nature 370 (1994) 621–628.
[2] K. Altendorf, W.P. Stalz, J.C. Greie, G. Deckers-Hebestreit, J. Exp. Biol. 203 (2000) 19–28.
[3] R. Birkenhäger, M. Hoppert, G. Deckers-Hebestreit, F. Mayer, K. Altendorf, Eur. J. Biochem. 230 (1995) 58–67.
[4] R. Birkenhäger, J.C. Greie, K. Altendorf, G. Deckers-Hebestreit, Eur. J. Biochem. 264 (1999) 385–396.
[5] B. Böttcher, L. Schwarz, P. Gräber, J. Mol. Biol. 281 (1998) 757–762.
[6] V.V. Bulygin, T.M. Duncan, R.L. Cross, J. Biol. Chem. 273 (1998) 31765–31769.
[7] B.D. Cain, R.D. Simoni, J. Biol. Chem. 263 (1988) 6606–6612.
[8] R.A. Capaldi, B. Schulenberg, J. Murray, R. Aggeler, J. Exp. Biol. 203 (2000) 29–33.
[9] P. Dimroth, G. Kaim, U. Matthey, J. Exp. Biol. 203 (1999) 51–59.
[10] P. Dimroth, H. Wang, M. Grabe, G. Oster, Proc. Natl. Acad. Sci. USA 96 (1999) 4924–4929.
[11] T.M. Duncan, V.V. Bulygin, Y. Zhou, L. Hutcheon, R.L. Cross, Proc. Natl. Acad. Sci. USA 92 (1995) 10964–10968.
[12] T. Elston, H. Wang, G. Oster, Nature 391 (1998) 510–513.
[13] R.H. Fillingame, W. Jiang, O.Y. Dmitriev, J. Exp. Biol. 203 (2000) 9–17.
[14] M.E. Girvin, R.H. Fillingame, Biochemistry 33 (1994) 665–674.
[15] M.E. Girvin, V.K. Rastogi, F. Abildgaard, J.L. Markley, R.H. Fillingame, Biochemistry 37 (1998) 8817–8824.
[16] P. Gräber, H.T. Witt, Biochim. Biophys. Acta 423 (1976) 141–163.
[17] L.P. Hatch, G.B. Cox, S.M. Howitt, J. Biol. Chem. 270 (1995) 29407–29412.
[18] S.M. Howitt, A.J.W. Rodgers, P.D. Jeffrey, G.B. Cox, J. Biol. Chem. 271 (1996) 7038–7042.
[19] H.F. Jäger, R. Birkenhäger, W.-D. Stalz, K. Altendorf, G. Deckers-Hebestreit, Eur. J. Biochem. 251 (1998) 122–132.
[20] A.T. Jagendorf, E. Uribe, Proc. Natl. Acad. Sci. USA 55 (1966) 170–177.
[21] W. Jiang, R.H. Fillingame, Proc. Natl. Acad. Sci. USA 95 (1998) 6607–6612.
[22] P.C. Jones, R.H. Fillingame, J. Biol. Chem. 273 (1998) 29701–29705.
[23] U. Junesch, P. Gräber, FEBS Lett. 294 (1991) 275–278.
[24] W. Junge, H. Lill, S. Engelbrecht, Trends Biochem. Sci. 22 (1997) 420–423.
[25] G. Kaim, P. Dimroth, Eur. J. Biochem. 218 (1993) 937–944.
[26] G. Kaim, P. Dimroth, Eur. J. Biochem. 222 (1994) 615–623.
[27] G. Kaim, F. Wehrle, U. Gerike, P. Dimroth, Biochemistry 36 (1997) 9185–9194.
[28] G. Kaim, U. Matthey, P. Dimroth, EMBO J. 17 (1998) 688–695.
[29] G. Kaim, P. Dimroth, Biochemistry 37 (1998) 4626–4634.
[30] G. Kaim, P. Dimroth, EMBO J. 17 (1998) 5887–5895.
[31] G. Kaim, P. Dimroth, FEBS Lett. 434 (1998) 57–60.
[32] G. Kaim, P. Dimroth, EMBO J. 18 (1999) 4118–4127.
[33] Y. Kato-Yamada, H. Noyi, R. Yasuda, K. Kinosita Jr., M. Yoshida, J. Biol. Chem. 273 (1998) 19375–319377.
[34] C. Kluge, P. Dimroth, Biochemistry 31 (1992) 12665–12672.
[35] C. Kluge, P. Dimroth, Biochemistry 32 (1993) 10378–10386.
[36] C. Kluge, P. Dimroth, J. Biol. Chem. 268 (1993) 14557–14560.
[37] W. Laubinger, P. Dimroth, Biochemistry 28 (1989) 7194–7198.
[38] W. Laubinger, G. Deckers-Hebestreit, K. Altendorf, P. Dimroth, Biochemistry 29 (1990) 5458–5463.
[39] R.N. Lightowlers, S.M. Howitt, L. Hatch, F. Gibson, G.B. Cox, Biochim. Biophys. Acta 894 (1987) 399–406.
[40] R.N. Lightowlers, S.M. Howitt, L. Hatch, F. Gibson, G.B. Cox, Biochim. Biophys. Acta 933 (1988) 241–248.
[41] J.C. Long, S. Wang, S.B. Vik, J. Biol. Chem. 273 (1998) 16235–16240.
[42] T. Masaite, N. Mitome, H. Noji, E. Muneyuki, R. Yasuda, K. Kinosita Jr., M. Yoshida, J. Exp. Biol. 203 (2000) 1–8.
[43] U. Matthey, G. Kaim, P. Dimroth, Eur. J. Biochem. 247 (1997) 820–825.
[44] U. Matthey, G. Kaim, D. Braun, K. Wüthrich, P. Dimroth, Eur. J. Biochem. 261 (1999) 459–467.
[45] D.T. McLachlin, S.D. Dunn, J. Biol. Chem. 272 (1997) 21233–21239.
[46] P. Mitchell, FEBS Lett. 43 (1974) 189–194.
[47] S. Neumann, U. Matthey, G. Kaim, P. Dimroth, J. Bacteriol. 180 (1998) 3312–3316.
[48] H. Noyi, R. Yasuda, M. Yoshida, K. Kinosita Jr., Nature 386 (1997) 299–302.
[49] O. Pänke, K. Gumbiowski, W. Junge, S. Engelbrecht, FEBS Lett. 472 (2000) 34–38.

[50] V.K. Rastogi, M. Girvin, Nature 402 (1999) 263–268.
[51] J. Reidlinger, V. Müller, Eur. J. Biochem. 223 (1994) 275–283.
[52] D. Sabbert, S. Engelbrecht, W. Junge, Nature 381 (1996) 623–625.
[53] Y. Sambongi, Y. Iko, M. Tanabe, H. Omote, A. Iwamoto-Kihara, I. Ueda, T. Yanagida, Y. Wada, M. Futai, Science 286 (1999) 1722–1724.
[54] H. Seelert, A. Poetsch, N. Dencher, A. Engel, H. Stahlberg, D.J. Müller, Nature 405 (2000) 418–419.
[55] S. Singh, P. Turina, C.J. Bustamante, D.J. Keller, R. Capaldi, FEBS Lett. 397 (1996) 30–34.
[56] K. Steffens, E. Schneider, G. Deckers-Hebestreit, K. Altendorf, J. Biol. Chem. 262 (1987) 5866–5869.
[57] D. Stock, A.G.W. Leslie, J.E. Walker, Science 286 (1999) 1700–1705.
[58] M. Takeyama, T. Noumi, M. Maeda, M. Futai, J. Biol. Chem. 263 (1988) 16106–16112.
[59] K. Takeyasu, H. Omote, S. Nettikadan, F. Tokumasu, A. Iwamoto-Kihara, M. Futai, FEBS Lett. 392 (1996) 110–113.
[60] W.S. Thayer, P.C. Hinkle, J. Biol. Chem. 250 (1975) 5330–5335.
[61] S.P. Tsunoda, R. Aggeler, H. Noji, K. Kinosita Jr., M. Yoshida, R.A. Capaldi, FEBS Lett. 470 (2000) 244–248.
[62] P. Turina, B.A. Melandri, P. Gräber, Eur. J. Biochem. 196 (1991) 225–229.
[63] F.I. Valiyaveetil, R.H. Fillingame, J. Biol. Chem. 273 (1998) 16241–16247.
[64] S.B. Vik, B.J. Antonio, J. Biol. Chem. 269 (1994) 30364–30369.
[65] S. Wilkens, R.A. Capaldi, Nature 393 (1998) 29.
[66] H. Yamada, Y. Moriyama, M. Maeda, M. Futai, FEBS Lett. 390 (1996) 34–38.
[67] Y. Zhang, R.H. Fillingame, J. Biol. Chem. 270 (1995) 87–93.